1988

Evaporation effects on the Mediterranean Sea mixed layer dynamics.

Turker, Ahmet

NAVAL POSTGRADUATE SCHOOL
Monterey, California

THESIS

EVAPORATION EFFECTS ON THE MEDITERRANEAN SEA MIXED LAYER DYNAMICS

by

Ahmet Turker

September 1988

Thesis Advisor — Roland W. Garwood
Co-Advisor — Pecheng Chu

Approved for public release; distribution is unlimited.

REPORT DOCUMENTATION PAGE

1a Report Security Classification: Unclassified		1b Restrictive Markings	
2a Security Classification Authority		3 Distribution/Availability of Report: Approved for public release; distribution is unlimited.	
2b Declassification/Downgrading Schedule			
4 Performing Organization Report Number(s)		5 Monitoring Organization Report Number(s)	
6a Name of Performing Organization: Naval Postgraduate School	6b Office Symbol (*If applicable*) 440	7a Name of Monitoring Organization: Naval Postgraduate School	
6c Address (*city, state, and ZIP code*): Monterey, CA 93943-5000		7b Address (*city, state, and ZIP code*): Monterey, CA 93943-5000	
8a Name of Funding/Sponsoring Organization	8b Office Symbol (*If applicable*)	9 Procurement Instrument Identification Number	
8c Address (*city, state, and ZIP code*)		10 Source of Funding Numbers	
		Program Element No / Project No / Task No / Work Unit Accession No	

11 Title (*Include security classification*): EVAPORATION EFFECTS ON THE MEDITERRANEAN SEA MIXED LAYER DYNAMICS

12 Personal Author(s): Ahmet Turker

13a Type of Report	13b Time Covered	14 Date of Report (*year, month, day*)	15 Page Count
Master's Thesis	From To	September 1988	70

16 Supplementary Notation: The views expressed in this thesis are those of the author and do not reflect the official policy or position of the Department of Defense or the U.S. Government.

17 Cosati Codes			18 Subject Terms (*continue on reverse if necessary and identify by block number*)
Field	Group	Subgroup	Ocean Mixed Layer Model, free convection , forced convection

19 Abstract (*continue on reverse if necessary and identify by block number*)

The OPBL (Oceanic Planetary Boundary Layer) model is used to determine the relative effects of the seasonally varying surface fluxes of heat, salt and momentum on the seasonal thermocline and mixed layer in the Mediterranean Sea. Three combinations of surface forcing are tested to find their relative contributions to mixing. In the first case free convection forcing and, in the second case wind forced convection and buoyancy flux due only to heat are considered to determine their individual effects on the mixed layer deepening. Then in the third case both free and wind forced convections are applied to the model in order to determine their combined effect on the mixed layer depth.

As a result, evaporation is shown to have a significant impact on the mixed layer deepening and on the temperature and salinity structure of the seasonal pycnocline. It has been shown that deepening due to evaporation exceeds the deepening due to wind stress between October and January. In the late winter the strong, cold, dry winds from North to Northwest (Mistral, Tramontane) causes forced convection which exceeds the deepening due to evaporation at this time of the year.

20 Distribution/Availability of Abstract ☒ unclassified/unlimited ☐ same as report ☐ DTIC users	21 Abstract Security Classification Unclassified	
22a Name of Responsible Individual Roland W. Garwood	22b Telephone (*Include Area code*) (408) 646-3260	22c Office Symbol 68 Gd

DD FORM 1473,84 MAR — 83 APR edition may be used until exhausted; All other editions are obsolete — security classification of this page

Approved for public release; distribution is unlimited.

Evaporation Effects On The Mediterranean Sea Mixed Layer Dynamics

by

Ahmet Turker
Lieutenant, Turkish Navy
B.S., Naval Academy, 1982

Submitted in partial fulfillment of the
requirements for the degree of

MASTER OF SCIENCE IN PHYSICAL OCEANOGRAPHY

from the

NAVAL POSTGRADUATE SCHOOL
September 1988

TABLE OF CONTENTS

ABSTRACT

The OPBL (Oceanic Planetary Boundary Layer) model is used to determine the relative effects of the seasonally varying surface fluxes of heat, salt and momentum on the seasonal thermocline and mixed layer in the Mediterranean Sea. Three combinations of surface forcing are tested to find their relative contributions to mixing. In the first case free convection forcing and, in the second case wind forced convection and buoyancy flux due only to heat are considered to determine their individual effects on the mixed layer deepening. Then in the third case both free and wind forced convections are applied to the model in order to determine their combined effect on the mixed layer depth.

As a result, evaporation is shown to have a significant impact on the mixed layer deepening and on the temperature and salinity structure of the seasonal pycnocline. It has been shown that deepening due to evaporation exceeds the deepening due to wind stress between October and January. In the late winter the strong, cold, dry winds from North to Northwest (Mistral, Tramontane) causes forced convection which exceeds the deepening due to evaporation at this time of the year.

LIST OF FIGURES

I. INTRODUCTION

A. PURPOSE OF THE STUDY

With respect to most oceanic basins, in the Mediterranean Sea we encounter some unique dynamic and physical characteristics. Such features as the vertical structure, general circulation, deep water formation and strait flows over the sills are unique to this inland sea. The Mediterranean Sea is an extreme case of thermodynamic interaction between atmosphere and the sea with the sea displaying strong reciprocal responses to the air-sea fluxes of mass and energy. Because of the large heat and radiation fluxes into the sea and excessive evaporation, the Mediterranean Sea is characterized by high salinities and temperatures, relative to oceanic water masses elsewhere.

The main purpose of this study is to understand the effects of strong evaporation and other seasonally varying atmospheric forcing on mixed layer dynamics in the Mediterranean Sea. To do this, the mixed layer model of Garwood (1977) was employed, using climatological forcing and analyses and forecasts from Fleet Numerical Oceanographic Center (FNOC). Model outputs are shown in Chapter IV in this thesis.

In Part (1B), the statement of problem is described. In the Part (1C), the literature is reviewed and summarized, in terms of the dynamic and physical characteristics and the general circulation of the Mediterranean Sea.

In the second chapter the equations on which the OPBL model was based are given. It is shown how from those equations a numerical solution is obtained to solve the initial value problem. The third chapter consists of observations and descriptive discussion. In the fourth chapter, the model simulations and results are shown. In the last chapter, conclusions and recommendations are presented.

B. STATEMENT OF PROBLEM

The upper layer of the sea responds to atmospheric forcing on seasonal, synoptic and diurnal time scales (Garwood, 1977). In this study, the Naval Postgraduate School Oceanic Planetary Boundary Layer Model (OPBL) was used for a variety of cases representative of atmospheric forcing in the Mediterranean Sea. Such cases include selective forcing of climatological values for wind stress, net evaporation minus precipitation (E-P) rate, and heat flux values to demonstrate individually the effect of seasonally varying variables on the Mediterranean mixed layer dynamics. The model was applied

at three stations which are purposely choosen because of their significant differences in atmospheric forcing, excess evaporation rate and general circulation with respect to each other.

In the Mediterranean Sea, convective processes play a very important role in the formation of Levantine Intermediate Water and deep water. In order to understand the water mass formation process within the Mediterranean Sea, we need to know the necessary driving mechanisms including wind forcing, heat and salt fluxes, thermohaline effects, vorticity and the effects of the general circulation. Due to the dry, cold wind experienced during the wintertime, the predominant mixing may be attiributed to convection cells reaching the deeper layers. The relative roles of wind stress and free convection for the mixing need to be evaluated quantitatively. An excess of evaporation over precipitation for the Mediterranean Sea requires that there be a net inflow through the Strait of Gibraltar to achieve mass balance (Garrett, 1983).

C. LITERATURE REVIEW

1. General Characteristics of The Mediterranean Sea

The vertical structure of the Mediterranean Sea consists of three water types:

(i) the surface Atlantic water,

(ii) Levantine Intermediate Water, and

(iii) the Mediterranean deep water.

Horizontally, the Mediterranean has two geographical regions: the western and eastern basins which are divided by a sill of 400 m depth extending from Sicily to the North African coast. The maximum depths are about 3400 m in the western basin and 4200 m in the eastern. The Levantine Intermediate Water is formed in the eastern basin during the winter off the south coast of Turkey with a temperature of 15 ° C and a salinity of 39.1 g/kg. It flows westward between 200 and 600 m depth along the North African coast and out below the surface through the Strait of Gibraltar into the Atlantic. In the Atlantic this intermediate water has a temperature and salinity that have been modified to 13 ° C and 37.3 g/kg, respectively, by mixing with overlying Atlantic water.

The outflow of Intermediate water below the surface is replaced by a surface inflow into the Mediterranean. Even though the western Mediterranean deep water extends from 100 m below the sill of Gibraltar to the bottom, it is surprising to find that both western Mediterranean deep water and Levantine Intermediate Water in the Atlantic. What can be the reasons for that? Bryden and Stommel (1982) mention the deep westward flow along the Moroccan continental slope with an anticyclonic gyre

deep westward flow along the Moroccan continental slope with an anticyclonic gyre which provides the high velocities necessary to raise the deep water up toward the Strait of Gibraltar. Also, high velocities in the Strait could provide an energy source to raise water from great depth up and over the sill. These high velocities are evident in the anticyclonic gyre in the Alboran Sea (Stommel, 1973).

In the Mediterranean Sea, evaporation exceeds precipitation plus river runoff. Therefore there is a net loss of fresh water which is made up by inflow of lesser salinity Atlantic water. For this Atlantic inflow process, the Mediterranean Sea water has a residence time of about 100 years.

2. Surface Forcing in Mediterranean

The wind stress at the sea surface generates turbulent kinetic energy which does work against the buoyancy forces, entraining the underlying denser water into the mixed layer and thus increasing the potential energy of the water column. The discontinuity in temperature and density that occurs at the bottom of the mixed layer is caused by the entrainment process, the rate of which is inversely proportional to the magnitude of the density jump.

Changes in the atmospheric pressure over the Mediterranean are the main driving mechanism for a significant part of low frequency sea level changes (Garrett, 1983). The wind-induced set-up outside the Strait of Gibraltar is less important than is atmospheric pressure in inducing flows through the Strait, except possibly for the high frequency response. The set-up on the shelf arises from a northward wind, which lags local atmospheric pressure by 90 °. So, the low frequency sea level changes, and Strait flows are found to be correlated with large scale meteorological forcing.

Bryden and Stommel (1984) suggest that the Mistral, which is a very strong, cold, dry continental wind from the northwest does not effect the deep water, unless a very strong buoyancy loss associated with wintertime convection exceeds a certain critical value.

According to the POEM (Physical Oceanography of the Eastern Mediterranean) group's report (Eos April 5, 1988), the eastern Mediterranean constitutes a general circulating basin in itself, including important wind and thermally driven components. In this basin, the convection processes produce the Levantine Intermediate Water (LIW) in the return flow toward Gibraltar. This flow forms the main body of the North Atlantic Upper Deep Water at intermediate depth in the Atlantic. The wind, thermohaline fluxes,

It is suggested that the Mistral can cause the convective mixing cells capable reaching the intermediate water (LIW) depth as well as deep layers in the southern Adriatic. They conclude that the wind-driven and the thermohaline components of the circulation are predominately driven by the air-sea latent and sensible heat fluxes in the eastern Mediterranean Sea where the general circulation is strongly seasonal.

In terms of overall mass balance it is expected that transport into the Mediterranean should exceed transport out of the Mediterranean, and the difference is balanced by the evaporation process over the entire Mediterranean Sea.

3. Deep water flow and formation in the Mediterranean Sea

In 1970, the Medoc Group proposed a first general description of Mediterranean deep water formation, divided into three consecutive phases:

(i) a preconditioning phase which is the erosion of the upper layer vertical stratification;

(ii) strong vertical mixing by meteorological forcing (usually caused by winds); and

(iii) sinking and spreading due to a baroclinic instability, producing small eddies.

In studying the formation of deep water in the northwestern Mediterranean Sea in winter, Gascard (1978) finds the frequent cyclonic and anticyclonic eddies are associated with processes of deep water formation. He suggests that a baroclinic instability is responsible for the slow current and the aperiodic vertical motions, and it is related to the formation of meanders, eddies, and fronts in the horizontal plane. Also, the northwest Mediterranean basin has been characterized during all seasons by a large cyclonic, thermohaline circulation of surface water masses coming from the Atlantic and subsurface water masses originating in the eastern Mediterranean (LIW) above a thick deep water layer (1500 to 2000 m). The Levantine Intermediate Water has been formed south of Turkey around the Islands of Rhodes and Cyprus with a maximum temperature and salinity value at a depth of about 150-300 m. During the winter the MEDOC area (northwestern Mediterranean Sea) is subjected to the effect of strong, cold, dry, continental winds from northwest to north (Mistral and Tramontane). High evaporation and strong cooling act to reduce the stability of the central part of the surface layer. There is a hydraulic control on the flows through the straits in combination with the evaporation over each of the basins, with the western Mediterranean surface water being 1.7 g/kg saltier than the Atlantic surface water, and the eastern Mediterranean 0.6 g/kg

g/kg saltier than the Atlantic surface water, and the eastern Mediterranean 0.6 g/kg saltier than the western Mediterranean. The deep water in the eastern Mediterranean appears to be formed in the Adriatic (Pollak, 1951), which is separated from the eastern basin by the Strait of Otronto. The MEDOC group remark that the deep water formation in the eastern basin is not a late-winter conversion of intermediate water into deep water, because the Adriatic is a separate basin with little intermediate water in its northernmost part.

According to Millot (1986) the fractional amount of water of Atlantic origin involved in the deep water formation processes occurring south of the French coast is roughly one-fourth (the other three-fourths being Levantine Intermediate Water) of the volume of water exiting from the Mediterranean Sea through the Strait of Gibraltar. So, the flow of LIW, although disturbed by various mesoscale phenomena, follows a steady cyclonic path along the continental slope off Italy, France and Spain, and it appears to be mainly forced by buoyancy. Deep water formation occurs during winter in the Gulf of Lions (Gascard, 1978). The reasons for the circulation inside the western Mediteranean Sea are not well understood at present. Lacombe *et al.*(1980) show that the density stratification in the Mediterranean Sea is controlled during the May-October warm season by the thermal structure. During the cold season it is controlled mainly by the salinity structure. In summer time the mean vertical motion is very weak. So the local deep water formation should occur during downward convective events of short duration. In the presence of large thermal losses in winter, due to high winds (Mistral and Tramontane) and dry cold air blowing over a warm sea, the density reached in the central area is greater than elsewhere, and convective motions are likely to start there first. This is called the *preconditioning phase*. During a strong mixing phase, high winds lasting for ten days and resulting in an evaporation rate of about 2 cm/day are able to homogenize the water down to 2000 m.

4. Mixing and Vertical Convection Processes in the Mediterranean

As in most temperate seas, the depth of the surface mixed layer is typically on the order of ten to one hundred meters, and the horizontal scale size is that of the internal Rossby radius, typically 12 to 15 km in the Mediterranean Sea.

Deepening of the mixed layer is caused by entrainment of the more dense underlying water into the turbulent region above. This process leads to a potential energy increase and cannot take place without the turbulent kinetic energy generated by

the wind stress and buoyancy loss at the surface of the mixed layer. Progressive cooling and evaporation which occur permanently in winter during periods of calm act on the quasi-homogeneous mixing zone and may induce a slow downward mean motion of new homogeneous and dense waters. This is the first process of deep water formation, it is called the *advective process.*

Also, strong and sudden surface cooling and evaporation produced by the *Mistral* or *Tramontane* acting on such a homogeneous and unstable structure may trigger intense deep convection within the interior of the fluid. This is called the *convective process*, and it causes the formation of new deep waters. A principal goal of this thesis research is to quantify the relative importance of wind-driven forced convection and buoyancy-driven free convection during this convective stage.

According to the Pollak (1951) the vertical convection currents can cause a complete overturning of the entire water column and can thus be an important factor in the formation of subsurface water characteristics which are most likely to occur during periods of minimum surface temperatures. Pollak also suggested that the Adriatic Sea, the only other possible source of deep eastern Mediterranean water, has a complicated structure. It is highly affected by the short-term weather fluctuations due to its restricted size and mean depth. Under those conditions the mixed water sinks and then flows sporadically along the bottom into the Mediterranean basin, where it circulates counterclockwise.

II. THEORY

A. OCEANIC PLANETARY BOUNDARY LAYER (OPBL) MODEL

1. General characteristics and dynamics of the OPBL

The OPBL model is a one-dimensional, second order turbulence closure, vertically integrated (bulk) model of the upper ocean surface turbulent boundary layer developed by Garwood (1977). It uses the continuity equation for an incompressible fluid, the first law of thermodynamics (heat equation), the conservation of salt equation, an analytical equation of state, the Navier-Stokes equation of motion with the geostrophic component eliminated, and a two-component vertically integrated turbulent kinetic energy (TKE) budget.

The oceanic boundary layer or mixed layer is the fully turbulent region that is bounded above by the air-ocean interface, and it is where the temperature and salinity are usually observed to be fairly well mixed. Below, the mixed layer is assumed to be bounded by a dynamically stable thermocline. It is assumed that the turbulence of the overlying mixed layer provides the energy needed to destabilize and erode the underlying stable thermocline in accordance with Garwood (1977). The wind and upward surface buoyancy flux through the surface are the sources of mechanical energy for the generation of this turbulence.

The model differs from earlier models: First, the amount of wind-generated TKE to be used in mixing is a function of the ratio of the mixed layer depth to the Obukhov mixing length L. Second, viscous dissipation is dependent on a local Rossby number. Finally, separate vertical and horizontal equations for TKE are used, permitting a more consistent interpretation of both entraining and retreating mixed layers.

This model shall be used to help understand the relative roles of wind stirring and surface buoyancy fluxes (attributable to both temperature and salinity fluxes) in the deep water formation for the Mediterranean Sea. In the following sections it is shown how to include salinity and the effects of strong evaporation in the theory for application to the Mediterranean Sea.

B. THE OPBL MODEL EQUATIONS

1. Temperature and Salinity Equations

Application of the first law of thermodynamics to mixed layer entrainment gives,

$$\delta T = -\Delta T \delta h / h. \tag{2.1}$$

Where δT is the mixed layer temperature reduction due to entrainment, ΔT is the discontinuity between the mixed layer temperature and the temperature immediately below the mixed layer. The mixed layer depth h is the distance over which turbulent energy must be transported by the vertical component of turbulent velocity.

The mixed layer temperature equation is therefore,

$$\frac{\partial T}{\partial t} = -\frac{\Delta T}{h}\frac{\partial h}{\partial t}. \tag{2.2}$$

The time derivative of h,

$$\frac{\partial h}{\partial t} = W_e - W_{(-h)} \tag{2.3}$$

is the entrainment velocity which depends on the vertical velocity,

$$\frac{\partial h}{\partial t} = W_e \tag{2.4}$$

where $W_{(-h)} = 0$.

Then the entrainment heat flux is

$$-\Delta T W_e = \overline{T'W'}_{(-h)}. \tag{2.5}$$

For mixed layer salinity, conservation of salt mass in the presence of entrainment yields a set of equations that are mathematically analogous to equation (2.1), equation (2.2) and equation (2.5):

$$\delta S = -\Delta S \delta h / h. \tag{2.6}$$

$$\frac{\partial S}{\partial t} = -\frac{\Delta S}{h}\frac{\partial h}{\partial t}. \tag{2.7}$$

$$\Delta S W_e = \overline{S'w'}_{(-h)}. \tag{2.8}$$

Here δS is the change in mixed layer salinity due to an entrainment increase of h by the depth increment δh, with ΔS being the salinity drop across the bottom of the

mixed layer. In equation (2.8), $\overline{S'w'}_{(-h)}$ is the entrainment salinity flux, and W_e is the same entrainment velocity invoked in equation (2.3) and equation (2.4).

Including the surface heat flux, equation (2.2) is augmented to become,

$$\frac{\partial T}{\partial t} = \frac{(Q_0/\rho C_p - \Delta T W_e)}{h}. \tag{2.9}$$

The mixed layer salinity budget equation (2.7) is similarly augmented to include the surface salinity flux, S(E-P), where E-P is the net evaporation minus precipitation rate:

$$\frac{\partial S}{\partial t} = \frac{S(E-P) - W_e \Delta S}{h}. \tag{2.10}$$

2. Buoyancy and momentum equations

The buoyancy equation is generated by the combination of the heat and salt equations with an equation of state,

$$\rho = \rho_0[1 - \alpha(\Delta T) + \beta(\Delta S)]. \tag{2.11}$$

where α and β are the expansion coefficients for heat and salt.

Buoyancy is defined as,

$$b = g\,\frac{(\rho_0 - \rho)}{\rho_0}, \tag{2.12}$$

where $b = B + b'$, decomposing into mean and turbulent parts.

The mean buoyancy equation is therefore derived from the heat and salt equations (2.9) and (2.10), using the equation of state (2.11) and the definition for buoyancy (2.12) :

$$\frac{\partial B}{\partial t} = -\frac{\partial \overline{b'w'}}{\partial z} + \frac{\alpha g Q}{\rho_0 C_p}. \tag{2.13}$$

By assuming the Boussinesq approximation, no viscous terms, incompressible fluid and subtracting the geostrophic equations from the total momentum equations, we obtain the mean momentum equations:

$$\frac{\partial U}{\partial t} = fV - \frac{\partial \overline{u'w'}}{\partial z} \tag{2.14}$$

$$\frac{\partial V}{\partial t} = fU - \frac{\partial \overline{v'w'}}{\partial z}. \tag{2.15}$$

Integration of (2.13), (2.14), and (2.15) over the entrainment zone gives us the jump conditions for the entrainment turbulent fluxes of buoyancy and momentum respectively:

$$-\overline{b'w'}_{(-h)} = \Delta B \frac{\partial h}{\partial t} \tag{2.16}$$

$$-\overline{u'w'}_{(-h)} = \Delta U \frac{\partial h}{\partial t} \tag{2.17}$$

$$-\overline{v'w'}_{(-h)} = \Delta V \frac{\partial h}{\partial t} \tag{2.18}$$

where

$$b' = \alpha g T' - \beta g S'$$

$$\Delta B = \alpha g \Delta T - \beta g \Delta S$$

$$\Delta T = \overline{T} - \overline{T}_{(-h-\delta)}$$

$$\Delta S = \overline{S} - \overline{S}_{(-h-\delta)}.$$

Here ΔT and ΔS are temperature and salinity discontinuity at the mixed layer base.

3. Mean Turbulent Kinetic Energy Equation

By subtracting the scalar product of (u,v,w) with the mean momentum equations from the mean kinetic energy equation we get the mean TKE equation:

$$\frac{1}{2}\frac{\partial \overline{E}}{\partial t} = -[\overline{u'w'}(\frac{\partial U}{\partial z}) + \overline{v'w'}(\frac{\partial V}{\partial z})] + \overline{b'w'} - \frac{\partial}{\partial z}\overline{[w'(\frac{p'}{\rho_0} + \frac{E}{2})]} - \varepsilon \cong 0. \tag{2.19}$$

(I) (II) (III) (IV)

where

$$E = u'^2 + v'^2 + w'^2. \tag{2.20}$$

The mixed layer turbulance is assumed to be in a quasi-steady state because the time rate of change TKE is usually smaller than the other terms and will be neglected. The term (I) represents the rate of mechanical production and is the dominant source of TKE for wind driven regimes. The term (II) represents the buoyancy flux and can be either a source or a sink. For strong evaporation and net surface heat loss $\overline{b'w'}$ will be large and positive and may become even more important than term (I) in producing mixed layer turbulence. The term (III) is the divergence of the turbulent flux of TKE and is responsible for transporting turbulence generated near the surface to the bottom of the mixed layer where it can cause entrainment and mixed layer deepening. The term (IV) represents viscous dissipation, the major loss of TKE.

The TKE equation in the entrainment zone, $z = -h$ is reduced to :

$$\frac{\partial}{\partial t}\left(\frac{\overline{E}}{2}\right)_{-h} = (-\alpha g \Delta T + \beta g \Delta S) W_e + \sqrt{w'^2}\,\frac{<\overline{E}>}{h}. \tag{2.21}$$

II III

In the entrainment zone, $\overline{E}$ generated higher in the layer is transported (by term III) into contact with the underlying water. When the TKE mixes this underlying water with the mixed layer water, at a rate W_e , the TKE is damped by the entrainment buoyancy flux (term II). In the entrainment zone (terms I and IV) are neglected, with the dominant balance assumed to be transport and buoyant damping.

4. Bulk Turbulence Equations

The resultant OPBL model equations may be summarized as follows:

Mixed layer depth:

$$\frac{\partial h}{\partial t} = W_e - \overline{W}_{(-h)}. \tag{2.22}$$

Entrainment rate, W_e, is derived from equation (2.21):

$$W_e = \frac{\sqrt{W'^2}\,<\overline{E}>}{h\alpha g \Delta T + <\overline{E}>}. \tag{2.23}$$

Equation (2.19) is integrated vertically to give total TKE for the mixed layer:

$$\frac{\partial}{\partial t}(h<\overline{E}>) = G_0 + G_h - B_0 - B_h - D. \tag{2.24}$$

The Vertical TKE component becomes :

$$\frac{\partial}{\partial t}(h<\overline{W'^2}>) = -B_0 - B_h + R - \frac{D}{3}. \tag{2.25}$$

Mixed layer currents are, equation (2.26) and equation (2.27):

$$\frac{\partial}{\partial t}(h<\overline{u}>) = fh<v> + \frac{\tau_x}{\rho}, \tag{2.26}$$

$$\frac{\partial}{\partial t}(h<\overline{v}>) = fh<u> + \frac{\tau_y}{\rho}. \tag{2.27}$$

Without salinity, the buoyant damping/production terms at the surface and at the bottom are:

$$B_0 = \alpha g h \overline{T'W'}(0) = -\alpha g h Q_0/(\rho C_p). \tag{2.28}$$

$$B_h = \alpha g h \Delta \overline{T} W_e. \tag{2.29}$$

With salinity effect, downward surface buoyancy flux, ΔB and B_h become respectively:

$$B_0 = [\alpha g[Q_0/(\rho C_p)] - \beta g \overline{S}(E - P)]h, \tag{2.30}$$

$$\Delta \overline{B} = \alpha g \Delta \overline{T} - \beta g \Delta \overline{S}, \tag{2.31}$$

$$B_h = (\alpha g \Delta T - \beta g \Delta S) W_e. \tag{2.32}$$

The shear production at the surface and at the bottom are :

$$G_0 = 12U^3 = 12[(\frac{\tau_x}{\rho})^2 + (\frac{\tau_y}{\rho})^2]^{3/4} \tag{2.33}$$

$$G_h = [<\overline{u}>^2 + <\overline{v}>^2] W_e. \tag{2.34}$$

Dissipation is modeled as,

$$D = 2 < \overline{E} >^{3/2}. \tag{2.35}$$

Redistribution, R in (2.25) is,

$$R = 2(< \overline{E} > -3 < \overline{w'^2} >)\sqrt{\overline{E}} \tag{2.36}$$

The following are the constants and the parameters which are needed in the model:

a. Model Constants

ρ_a Density of air

ρ_0 Density of sea water

α Thermal expansion coefficient

β Haline expansion coefficient

g Acceleration of gravity

C_p Specific heat at constant pressure

C_D Drag coefficient

b. Model Parameters

f Coriolis parameter

τ Wind Stress

Q_0 Incoming solar radiation

Q_b Longwave back radiation

Q_e Latent heat flux

Q_h Sensible heat flux

E Evaporation rate

P Precipitation rate

5. Approximation For Entrainment Equation

a. Preliminary Assessment of Effects of Evaporation

The Garwood (1977) model system equations (2.22) to (2.36) may be approximated by the Krauss-Turner (1967) model, which neglects dissipation (D) and entrainment shear production (G_h):

$$W_e = (G_0 - B_0)/\Delta B \tag{2.37}$$

b. Steady-State Non-Entraining Mixed Layer (Spring and Summer)

If B_0 is positive and equals G_0, then there is no entrainment, $W_e = \partial h/\partial t = 0$, and $B_0 = G_0$, or

$$[\alpha g(\frac{Q_0}{\rho} C_p) - \beta g \bar{S}(E - P)]h = G_0. \tag{2.38}$$

Solving for the steady-state diagnostic mixed layer depth in equation (2.38) gives:

$$h = \frac{G_0}{[\alpha g Q_0/\rho C_p - \beta g \bar{S}(E - P)]} \tag{2.39}$$

It is readily seen that a net $(E - P) > 0$ will reduce the denominator, increasing h. In addition to an obvious increase in mixed layer salinity due to evaporation, the mixed layer temperature will be indirectly changed by the increase in h. So this latter effect, equation (2.8) is combined with equation (2.39) with $W_e = 0$,

$$\frac{\partial T}{\partial t} = \frac{Q_0/(\rho C_p)}{[G_0/\alpha g Q_0/\rho C_p - \beta g \bar{S}(E - P)]}. \tag{2.40}$$

In the numerator of equation (2.40) evaporation decreases Q_0 directly due to the loss of latent heat. But, the accompaning increase in mixed layer depth will further reduce mixed layer temperature by increasing the denominator of the right-hand side of equation (2.40). Thus it has been shown that we should expect the surface salinity flux due to E to indirectly influence the evolution of the temperature profile, as well as the evolution of the salinity profile.

c. Deepening Mixed Layer (Fall and Winter)

During the fall and winter, the mixed layer deepens and $W_e \neq 0$. Therefore the complete model equations must be solved. Nevertheless, the effects of $W_e > 0$ may be seen in the heat and salt equations (2.6) and (2.10). The general tendency for change in mixed layer temperature due to a strong evaporation will be due to two contributions:

(i) Q_0 will be made more negative due to the loss of latent heat,

(ii) h and W_e will be increased due to the increased production of TKE by the extra surface buoyancy flux. In the Mediterranean ΔT will almost always be positive, so enhanced entrainment will always reduce the mixed layer temperature.

In the mixed layer salinity budget, equation (2.10), the net effect of strongly positive (E-P) is to increase mixed layer salinity. Whereas, equation (2.10) shows that the increase is not as great as it will be for a constant-depth mixed layer (as in the summer). The $-W_e\Delta S$ term of equation (2.10) will usually reduce mixed layer salinity because ΔS will generally be positive during the fall and winter. However, it may be negative in some locations, especially if there is strong horizontal advection with higher salinity, water interleaving below the mixed layer. Also, $(E-P)>0$ increases h, reducing the magnitude of $\partial S/\partial t$.

III. OBSERVATIONS AND DESCRIPTIVE DISCUSSION

A. OBSERVED SURFACE HEAT FLUX CHARACTERISTICS

In our problem daily heat and radiation fluxes are provided from the climatology of Hsiung (1983, 1985) for the three locations of interest in the Mediterranean Sea.

The net surface heat flux can be written as,

$$Q_0 = Q_s - Q_e - Q_h - Q_b \tag{4.1}$$

where

Q_s Incoming Solar Radiation,

Q_e Upward Latent Heat Flux

Q_h Upward Sensible Heat Flux

Q_b Outgoing Longwave Radiation

The latent heat flux proportional to E,

$$Q_e = \rho L E \tag{4.2}$$

where the evaporation rate E in cm/day is also available from climatological data.

The fluxes of radiation, latent and sensible heat at the sea surface determines shallowing or deepening of the mixed layer by entrainment. According to the equations (2.33), (2.36) and (2.39), if there is a positive buoyancy flux ($Q_0 < 0$ and ($E > P$) then the mixed layer must deepen. This will be the case at night or whenever longwave radiative cooling plus the upward turbulent fluxes of heat exceed solar radiation. The negative downward buoyancy flux will result in the shallowing of the MLD provided wind stress is not large.

In the Mediterranean, with large (E-P), it may be possible to have a net downward heat flux, $Q_0 > 0$, and still have a net upward surface buoyancy flux. From equation (2.30), $B_0 < 0$ whenever

$$[\alpha g \frac{Q_0}{\rho C_p} - \beta g \bar{S}(E - P)] < 0$$

Solving the inequality for E-P, this situation will occur if,

$$(E-P) > [\frac{\alpha \rho C_p Q_0}{\beta \bar{S}}]. \tag{4.3}$$

This effect may be particularly important during the late winter or early spring when Q_0 may be positive, but small. If this were to happen, the surface buoyancy flux would be positive, producing added TKE to possibly deepen the mixed layer well beyond the maximum depth possible for a temperature-dominant ocean. This process could also be an important mechanism to mix heat downward, overcoming the normal stratifying tendency of the surface heat flux.

The distribution of the surface heat flux does not have significant differences over Mediterranean from place to place. However, the large evaporation rate over the Mediterranean is very unusual and it causes the strong turbulent mixing in the surface boundary layer. Due to the similar surface heat flux values over the Mediterranean Sea we do not expect significantly different results in terms of the mixed layer dynamics between three stations which are chosen in the Mediterranean Sea.

From Fig. 1 on page 18, Fig. 2 on page 19, Fig. 3 on page 20, and Fig. 4 on page 21, we see the latent heat flux and incoming solar radiation values at two stations in the central and western Mediterranean, respectively.

At the eastern Mediterranean Station ($\phi = 35°N, \lambda = 30°E$), the latent heat flux decreases from the initial value which is 165 W/m^2 to 43 W/m^2 in winter. After May, it increases until end of the year. After the middle of October, the latent heat flux increases sharply, probably due to the large air-sea temperature difference. Depending on the latent heat flux, evaporation contributes to the buoyant production of TKE and causes vertical mixing. Therefore, at this station the TKE is enhanced by evaporation the most during November.

Incoming solar radiation is almost a sinusoidal curve over the year. See Fig. 5 on page 22. It increases smoothly from the January value 81 W/m^2 until July, then decreases smoothly until end of the year.

Fig. 7 on page 24 shows the net heat flux. From January to July it increases from -183 W/m^2 to 211 W/m^2, and it then decreases to -200 W/m^2 in December.

At the central Mediterranean station ($\phi = 35°N, \lambda = 20°E$) , Fig. 2 on page 19 the latent heat flux differs from that at the eastern station. At this station, latent heat flux peaks in February, then decreases until the middle of the June. It then increases through

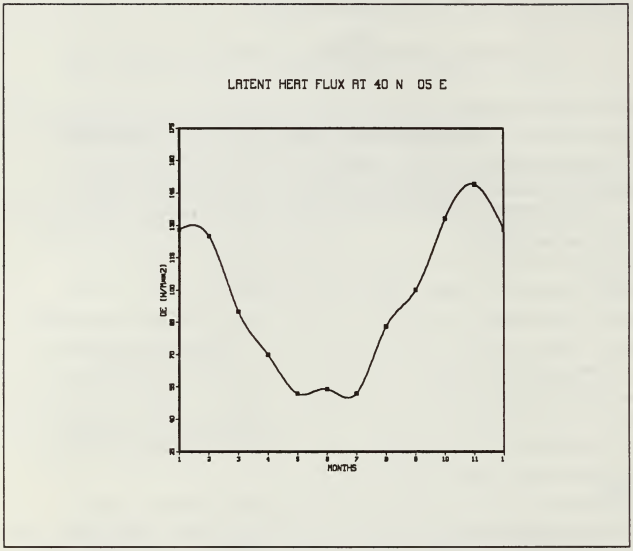

Fig. 1. The Latent Heat Flux At 40 ° N 05 ° E

October, with an unusual plateau in August and September. After October it decreases to 144 W/m^2.

Incoming solar radiation in central part of Mediterranean differs from in the eastern part only slightly. Also the net downward heat flux is similar to that in the eastern Mediterranean.

In the western Mediterranean, Fig. 1 shows the latent heat flux. From January to May, latent heat flux and, therefore, evaporation rate gets smaller. It then increases slightly in June. Between June and July it decreases slightly. From July until November, latent heat flux increases sharply, then decreases until end of the year. The maximum latent heat flux is in November. Minima are in May and July.

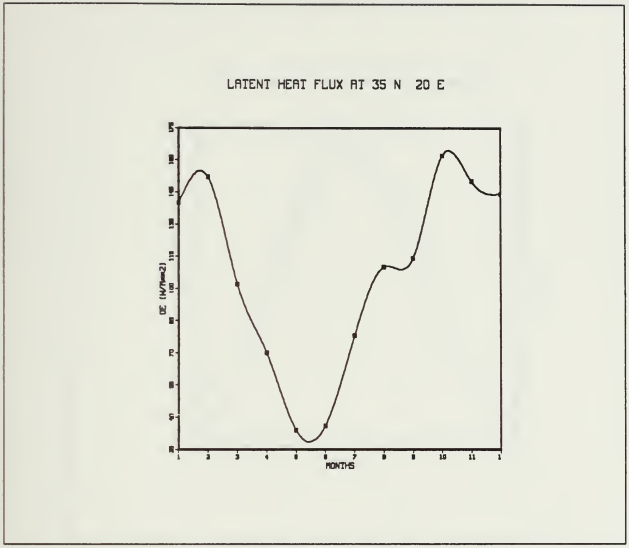

Fig. 2. The Latent Heat Flux At 35 ° N 20 ° E

Incoming solar radiation is similar to the other stations. See Fig. 3 on page 20, Fig. 4 on page 21 and Fig. 5 on page 22.

B. THE OBSERVED WIND STRESS DISTRIBUTION

The wind stress values are computed from climatological wind speed data. The drag coefficient, C_D depends upon the wind speed climatology and the formulation of Bunker (1976).

As for the surface heat fluxes, the wind velocity values don't differ significantly for the different locations. However, the western station has somewhat stronger wind speeds than does the eastern Mediterranean. See Fig. 8 on page 25, Fig. 9 on page 26, and Fig. 10 on page 27.

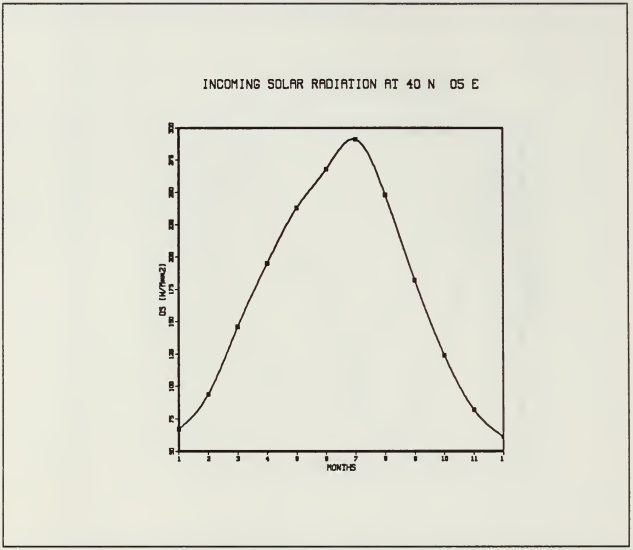

Fig. 3. The Incoming Solar Radiation At 40 ° N 05 ° E

From seasonal variations in the wind, we subdivide the year into three periods. In the first period, (between January and June in western and central Mediterranean, but from January to May in eastern Mediterranean), wind stress generally is decreasing. In the second period which is in summer, wind speeds are lowest. This period lasts usually until September. Then in the third portion of the year, wind stress increases continually. So, the maximum wind stress occurs between November and April, and the minimum occurs between May and October.

Fig. 8 on page 25, Fig. 9 on page 26 and Fig. 10 on page 27 show the wind velocity as functions of time for the selected stations in the Mediterranean Sea.

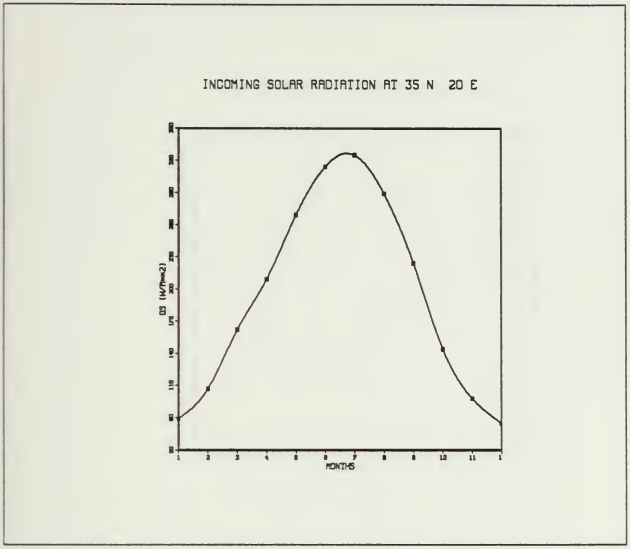

Fig. 4. The Incoming Solar Radiation At 35 ° N 20 ° E

C. OBSERVED TEMPERATURE AND SALINITY CHARACTERISTICS

The eastern Mediterranean basin is isolated from the western basin by the Strait of Sicily. The Eastern basin experiences some important wind and thermal forcing. Due to convection processes, the salty Levantine Intermediate Water is produced here. This water mass (LIW) flows into the Atlantic Ocean, and it forms the main body of the North Atlantic upper deep water. (Malonette *et al.*, 1988). Understanding the formation of this water mass is therefore important for the Atlantic, as well as the local thermohaline circulations. The eastern Mediterranean has a maximum depth, surface temperature and salinity, 4200 m, 26 ° C and 39.1 g kg., respectively. Fig. 11 on page 28 shows the observed temperature structure in the eastern Mediterranean Sea. As can

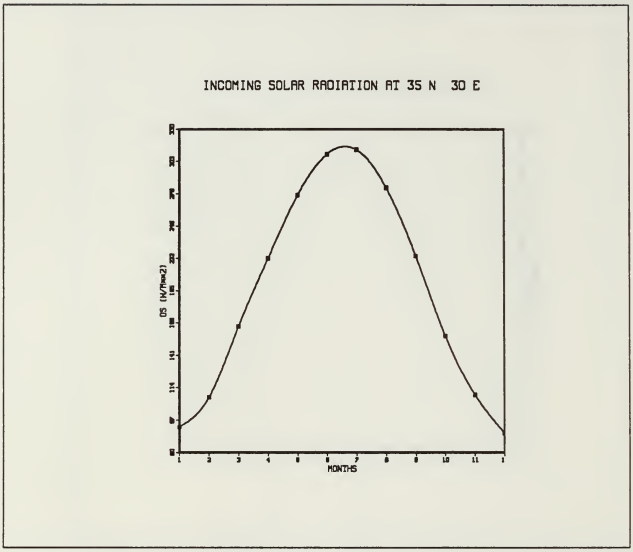

Fig. 5. The Incoming Solar Radiation At 35 ° N 30 ° E

be seen from the complete picture, the oceanographic year can be considered as having a cool season from November to April and warm season from May to October. During the warm season, mixed layer temperature increases, and the 16.5 ° C isotherm rises to 170 m depth due to the surface heating and calm weather conditions. Below the 170 m depth the vertical structure is most stratified. In the cool season, the surface layer experiences strong wind effects and surface cooling due to atmospheric winter conditions and excessive evaporation rate. Therefore, buoyancy loss causes vertical mixing within the surface boundary layer, and this mixing can penetrate to a depth of 1200 m. See Fig. 12 on page 29.

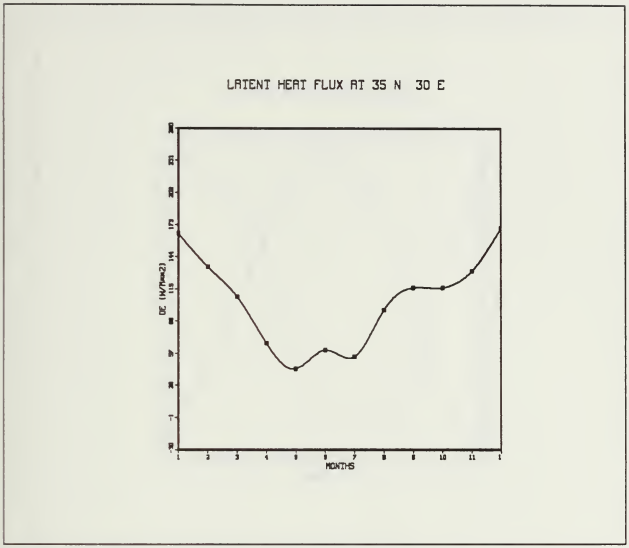

Fig. 6. The Latent Heat Flux At 35 ° N 30 ° E

At the central Mediterranean Sea station, ($\phi = 35°N, \lambda = 20°E$) the mixed layer temperature drops due to winter atmospheric conditions. The MLD deepens below 100 m. In summer, due to calm weather conditions and excess downward heat flux, mixed layer temperature increases and is accompanied by a significant reduction in MLD.

The most significant differences between the central and the eastern Mediterranean temperature structure are attributable to the differences in surface heat flux in the eastern Mediterranean relative to the surface heat flux in the central regime. There are higher temperatures at all depths in the eastern regime relative to the central. See Fig. 12 on page 29 and Fig. 13 on page 30. Another significant difference is that the wind stress in

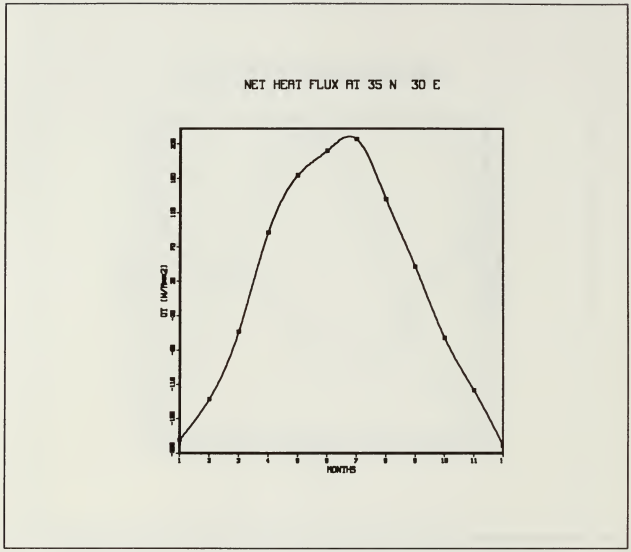

Fig. 7. The Net Heat Flux At 35 ° N 30 ° E

the central regime is stronger than in the eastern regime in any month of the year. These two atmospheric forcing factors play a very important role in the mixed layer dynamics.

From Fig. 14 on page 31, the surface salinity value is highest between May and October, probably due to relatively warmer and calm wind conditions, coupled with higher evaporation rate.

The shallow summer time mixed layer is responsible for this increase in surface salinity. The strong evaporation continues in spite light winds. However, the light winds (small G_0) and strong insolation (large Q_0) cause the mixed layer to be shallow, concentrating the salinity in a small volume. This is predicted by equation (2.24) :

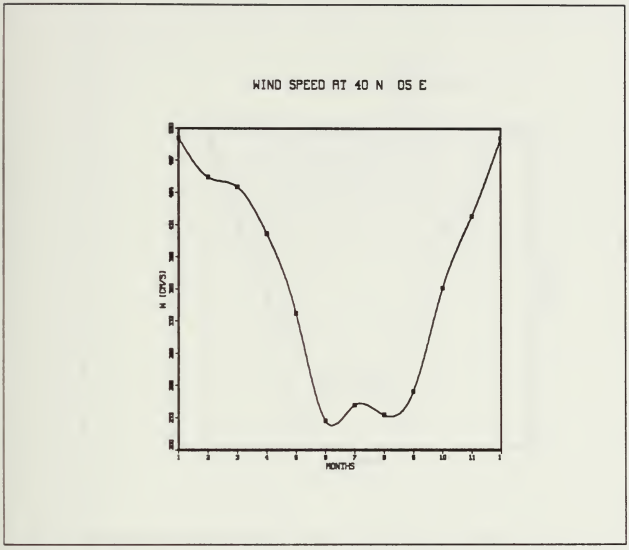

Fig. 8. The Wind Velocity At 40 ° N 05 ° E

$$h = \frac{G_0}{[\alpha g Q_0 / \rho C_p - \beta g \bar{S}(\bar{E} - \bar{P})]} .$$

Here $\bar{E} - \bar{P}$ is insufficiently large to overcome Q_0 , and the inequality (4.3) is not yet satisfied :

$$(E - P) < < \alpha g \frac{Q_0}{\beta \rho C_p \bar{S}} .$$

However, as fall comes on and Q_0 is reduced, the dominant buyancy flux contribution shifts from Q_0 to (E-P). This salty but warm surface water cools in fall and be-

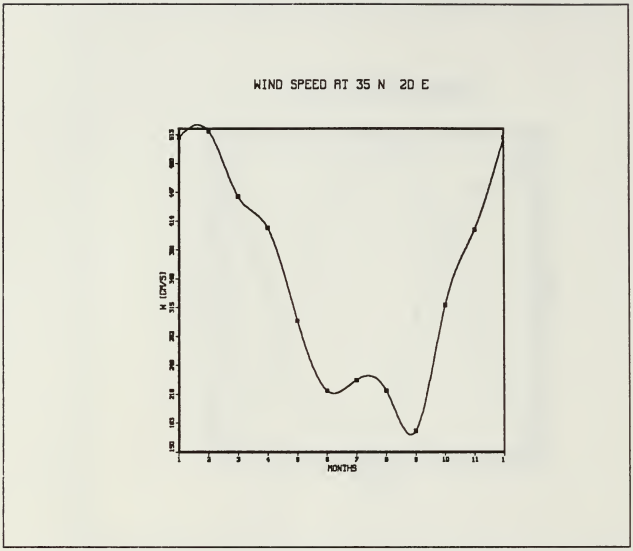

Fig. 9. The Wind Velocity At 35 ° N 20 ° E

comes denser than the water below, and it sinks. Fig. 14 on page 31 shows an example of convected surface water with a core depth of 210 m and 160 m. As is suggested by Malanotte-Rizzoli and Robinson (1987), the Mistral and Tramontone winds which are strong, cold and dry can start the mixing process, called the *preconditioning phase* . This can overturn the water column down to a couple of hundred meters depth. This process is equivalent to the formation process of Levantine Intermediate Water in the eastern Mediterranean which was also suggested by Bryden and Stommel (1983).

Unlike the eastern Mediterranean, salinity increases with depth in the central Mediterranean. See Fig. 15 on page 32 and Fig. 16 on page 33. This reduction in temperature and increase in salinity with depth makes the vertical water structure very stable

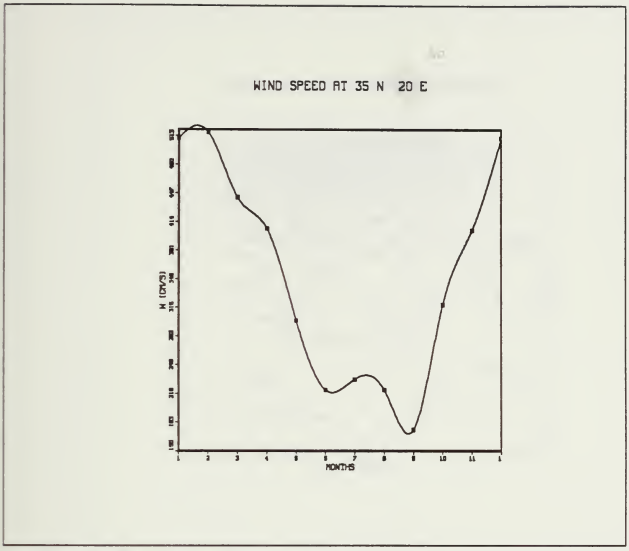

Fig. 10. The Wind Velocity At 35 ° N 30 ° E

in this part of the Mediterranean Sea. Due to such a stable vertical structure in the central Mediterranean Sea, the mixing process can only be significant during the strong wind storms in winter associated with the Mistral and Tramontone.

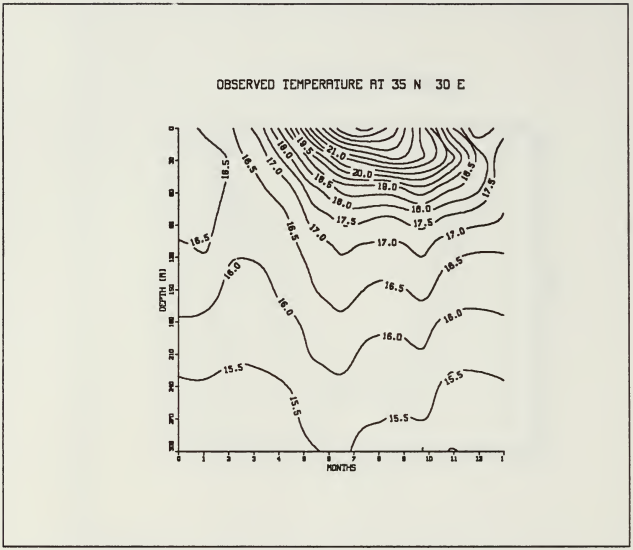

Fig. 11. The Observed Temperature At 35 ° N 30 ° E

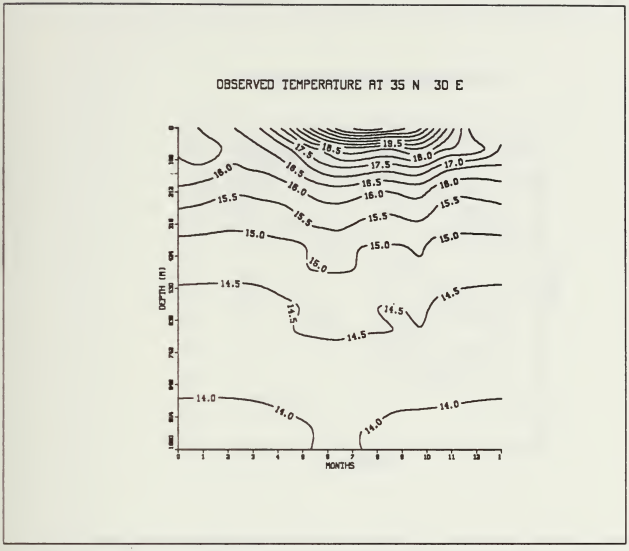

Fig. 12. The Observed Temperature At 35 ° N 30 ° E

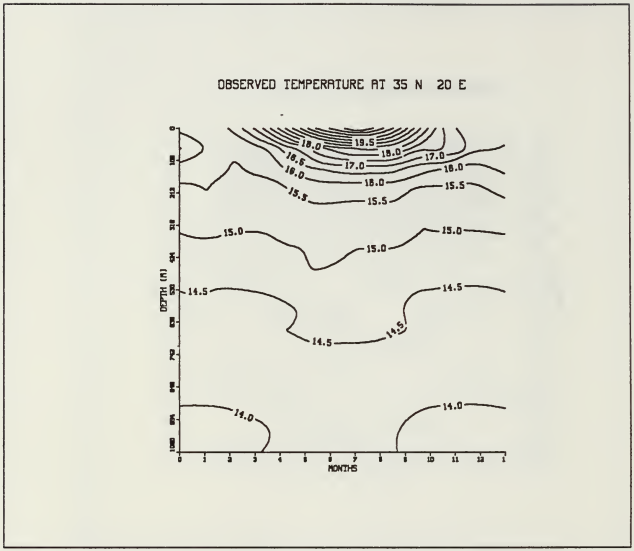

Fig. 13. The Observed Temperature At 35 ° N 20 ° E

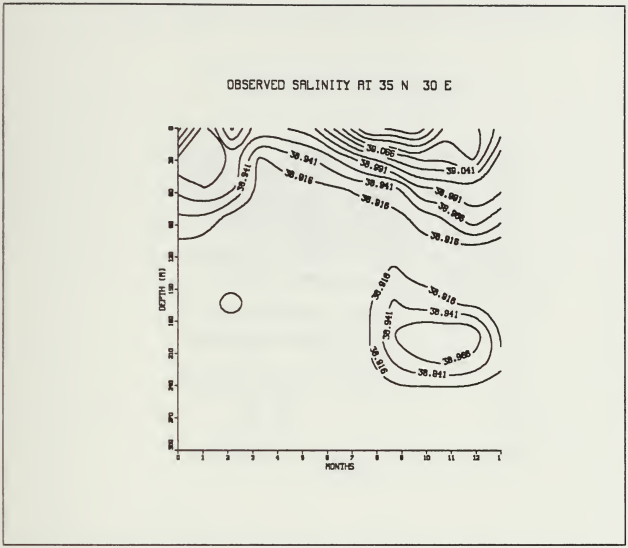

Fig. 14. The Observed Salinity At 35 ° N 30 ° E

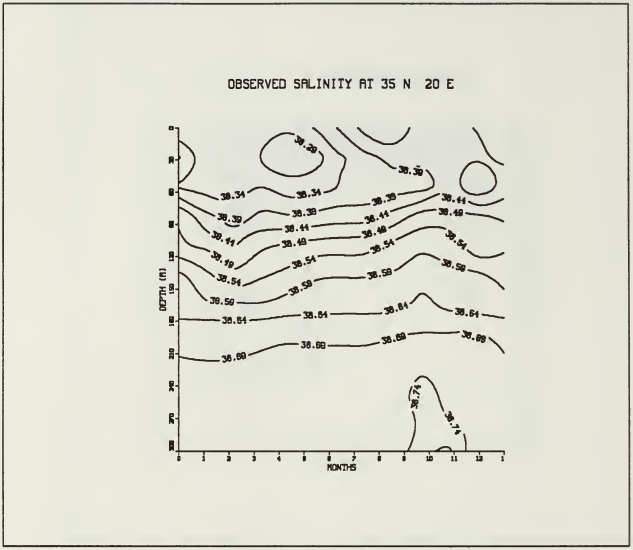

Fig. 15. The Observed Salinity At 35 ° N 20 ° E

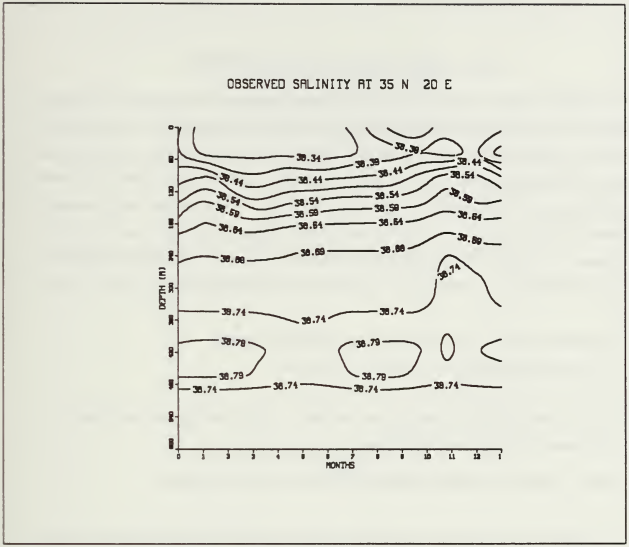

Fig. 16. The Observed Salinity At 35 ° N 20 ° E

IV. OPBL MODEL SIMULATIONS

The OPBL Model is used to study the relative importance of evaporation, heat flux, and wind stress for mixing at three stations in the Mediterranean Sea. The monthly heat flux data for these Mediterranean locations were obtained from the climatological data computed by Hsiung (1983, 1985), and the wind stress data were provided from wind stress climatology. (U.S. Navy Marine Climatic Atlas). The specified daily boundary conditions are latent heat flux (Q_e) , incoming solar radiation (Q_s), net heat flux (Q_i) , wind stress (τ), evaporation (E), and precipitation (P). The predicted model variables are mixed layer depth (h), temperature (T), salinity (S), and below-layer profiles T(z) and S(z).

The model is run at the three locations, using three cases:

(i) free convection (heat and salinity fluxes) only ;

(ii) forced convection plus heat flux only ; and

(iii) combined free and forced convection (heat, salinity and momentum fluxes)

A discussion of model results follows.

A. CASE 1 (FREE CONVECTION ONLY, NO WIND STIRRING)

The purpose of this case is to show the effect of excessive evaporation over precipitation without wind effects on the mixed layer dynamics at all three stations. One can see the correlation between net heat flux Fig. 17 on page 35 and mixed layer depth Fig. 18 on page 36.

For the case where the evaporation exceeds precipitation in the eastern Mediterranean, creating a net evaporation, the mixed layer temperature changes depend on the seasonally varying net heat flux. In January mixed layer depth deepens from initial depth (95 m) to 197 m. After January mixed layer depth is constant at 197 m until the second half of April. At the end of April the mixed layer shallows rapidly to 0 m, and sudden fluctuations occur in May. After the second half of May, the mixed layer depth shallows to the surface and remains at the surface over the summer. After the second half of October, mixed layer depth again deepens until end of the year to 120 m, due to vertical overturning caused by net surface cooling plus the buoyancy loss attributable to the evaporation rate.

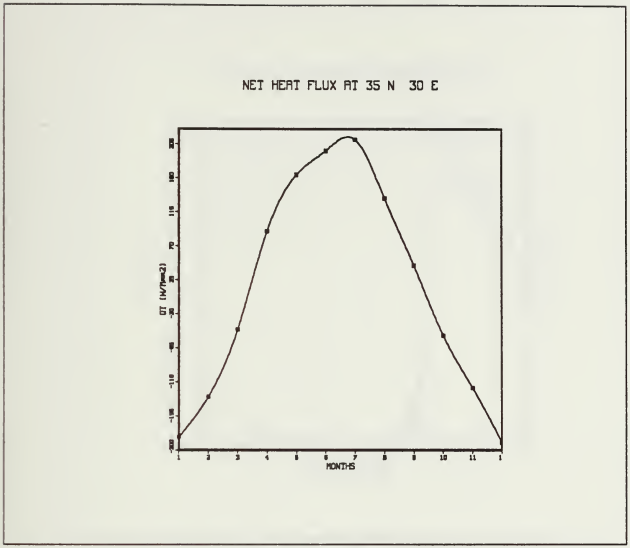

Fig. 17. The Net Heat Flux At 35 ° N 30 ° E

turning caused by net surface cooling plus the buoyancy loss attributable to the evaporation rate.

Because of evaporation, the salinity increases at first according to equation (2.10). In January and fall the predicted mixed layer deepening is due to the reduction in the downward surface buoyancy flux, causing a deeper h. As evaporation continues, the surface water gets saltier and denser than the water lying immediately below. As a result, the denser surface water sinks until reaching the same density. Strong positive (E-P) increases mixed layer salinity by increasing the numerator of the equation (2.10). This increase in E-P increases the mixed layer depth by decreasing the denominator of equation (2.39):

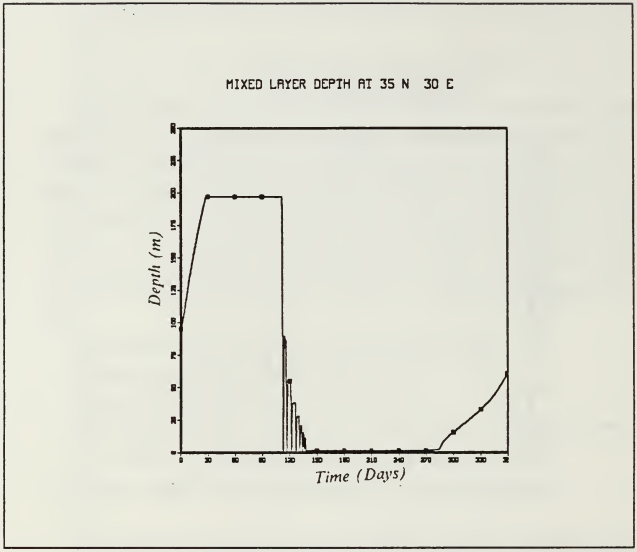

Fig. 18. The Mixed Layer Depth With Free Convection Only

$$h = \frac{G_0}{[\alpha g Q_0/\rho C_p - \beta g \bar{S}(E-P)]}.$$

See Fig. 19 on page 37 and Fig. 20 on page 38.

In the central Mediterranean, the mixed layer structure is very similar to the eastern, with only slight differences at corresponding depths. The mixed layer deepens to 197 m depth at this location in January and it stays at the same depth between February and May as in the eastern Mediterranean. In April, the mixed layer shallows rapidly to the surface and then stays constant until the middle of October. After October the mixed layer depth deepens to 90 m until the end of December. See Fig. 21 on page 39.

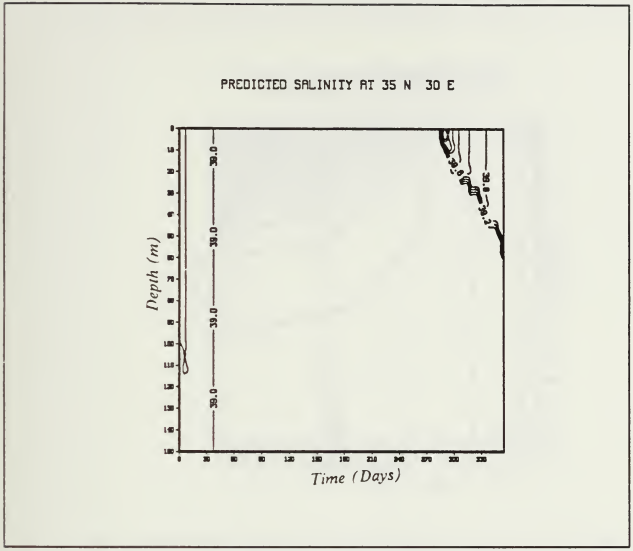

Fig. 19. The Predicted Salinity With Free Convection Only

As for the eastern and central Mediterranean mixed layers, the western Mediterranean mixed layer depth is well-correlated with the net heat flux variations. Going from the eastern to the western Mediterranean, the rate of late winter and early spring mixed layer deepening does not change and stays constant at 197 m in April. Conversely, the rate of mixed layer deepening increases at the end of the year from 60 m to 125 m, as we go from eastern to western Mediterranean. See Fig. 18 on page 36, Fig. 21 on page 39, and Fig. 22 on page 40.

B. CASE 2 (THE EFFECT OF THE WIND STRESS ON MLD WITHOUT E-P)

Fig. 24 on page 42 depicts the mixed layer depth versus time in the eastern Mediterranean. The mixed layer depth deepens from initial depth (95 m) to 197 m in

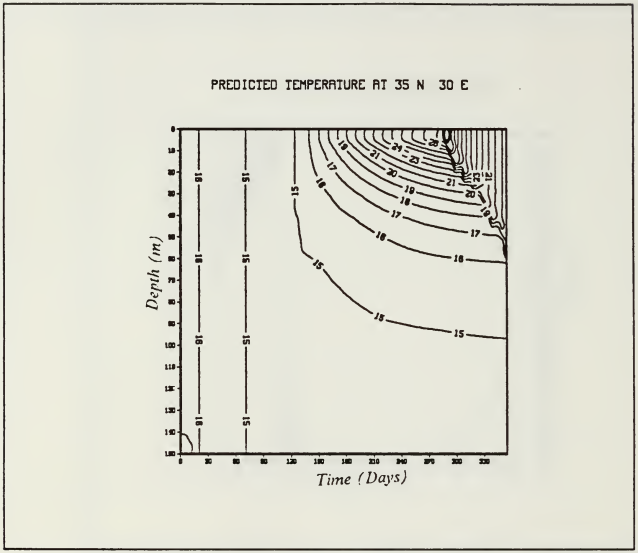

Fig. 20. The Predicted Temperature With Free Convection Only

January in the forced convection plus heat flux case and then stays constant between February and May at 197 m as in the free convection plus heat and salinity fluxes case. In April there is a sharp shallowing with a small fluctuation. Then MLD becomes constant at about 10 m depth until September. Between October and January, the mixed layer deepens to 43 m. In April there is a large sharp decrease and then a small sharp increase in mixed layer depth. This is probably due to a rapid changes in wind stress and surface buoyancy fluxes. Also, one can see the correlation between mixed layer temperature and wind velocity. See Fig. 25 on page 43 and Fig. 26 on page 44. From Fig. 27 on page 45, Fig. 24 on page 42, and Fig. 28 on page 46, we can see the similarity between the mixed layer depth plots.

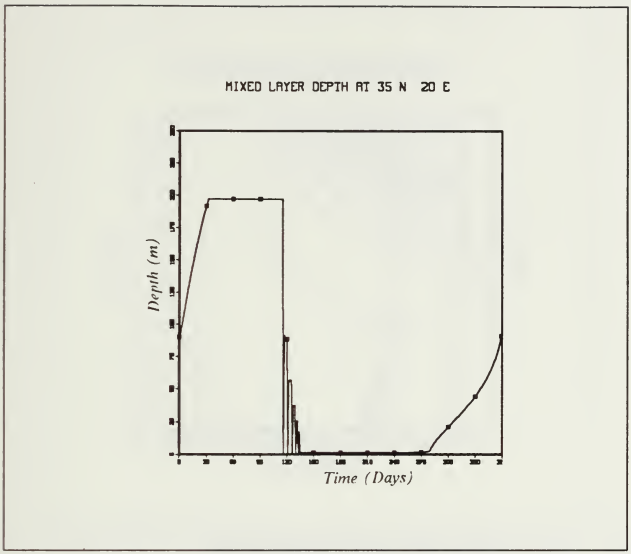

Fig. 21. The Mixed Layer Depth With Free Convection Only

In the central Mediterranean Sea, the mixed layer deepens until the middle of February to 197 m. Then it stays constant until the end of March. After March, MLD shallows sharply with a small fluctuation in April until July. During the summer, the mixed layer depth is less than 6 m. Due to the stronger wind conditions here the mixed layer depth deepens between October and January to 56 m depth.

Mixed layer deepening ends in February in the western Mediterranean Sea as at the other locations, due to increased insolation. Shallowing starts in late March, and it continues until July at around 10 m depth. Then the mixed layer remains constant until September at 10 m depth, and then it deepens to 90 m at the end of the year due to the

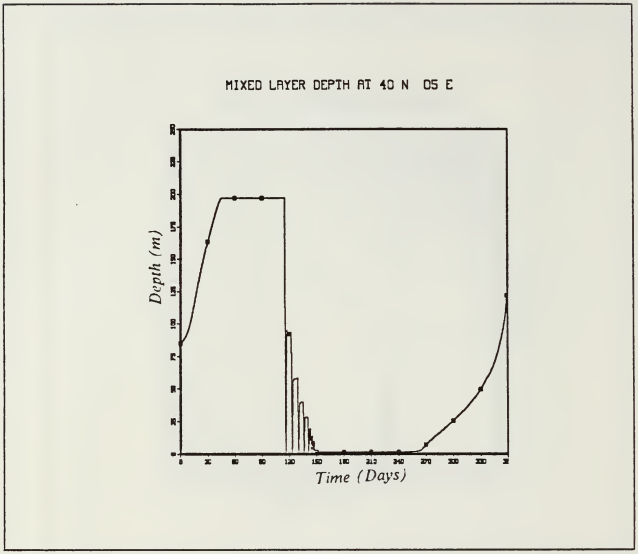

Fig. 22. The Mixed Layer Depth With Free Convection Only

relatively short time period of strong winter winds. See Fig. 34 on page 52 and Fig. 28 on page 46.

C. CASE 3 (COMBINED FREE AND FORCED CONVECTION)

In this case the model is forced by the combination of wind, heat fluxes and evaporation. Between October and March the mixed layer can deepen more than in the first two cases alone due to the combination of strong wind and evaporative conditions. During the fall and winter cooling period, the mixed layer cools and deepens. Part of the cooling is due to surface heat loss, and part is attributable to the entrainment of underlying cold water. The seasonal thermocline weakens, and it usually vanishes by March. During the heating period, net heat gained in daytime is retained through the

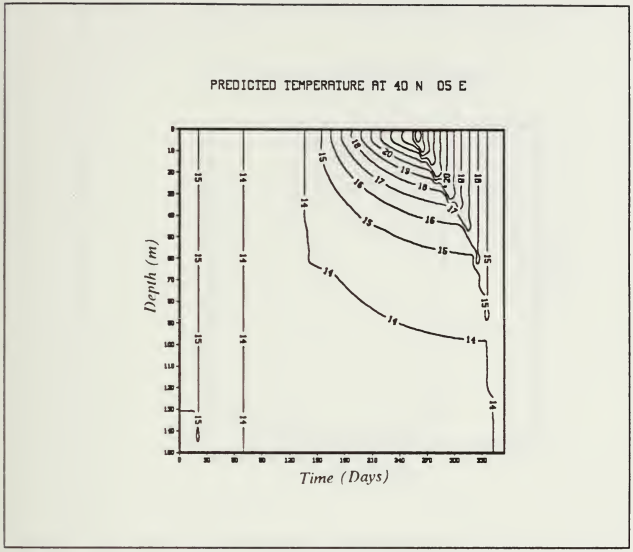

Fig. 23. The Predicted Temperature With Wind And Heat Fluxes Only

night, so there is a cumulative gain. Fig. 29 on page 47, Fig. 32 on page 50, Fig. 30 on page 48, and Fig. 31 on page 49 show mixed layer depth, mixed layer temperature and salinity, and incoming solar radiation versus time, respectively, for the eastern Mediterranean Sea.

D. RESULTS

The most significant results may be summarized for the above cases. Whenever the evaporation becomes largest, the mixed layer depth becomes deepest in the case of free convection forcing only. Depending on the latent heat flux, evaporation is largest in winter in the eastern Mediterranean. See Fig. 33 on page 51. One can see that the mixed layer depth reaches its maximum value after the late winter peak in the latent heat flux

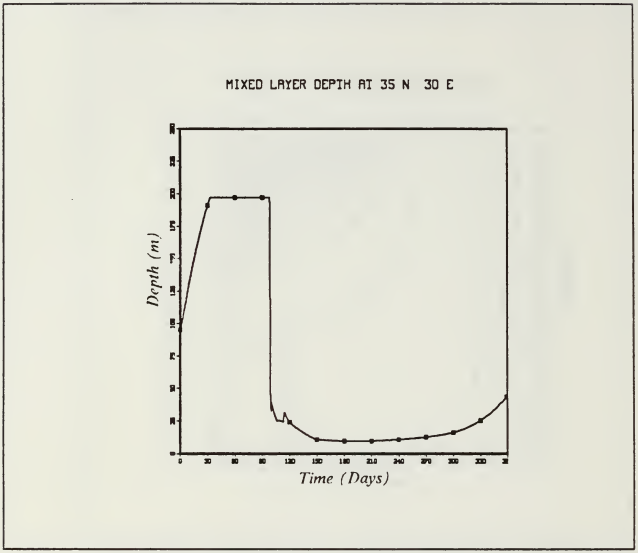

Fig. 24. The Mixed Layer Depth With Wind And Heat Fluxes Only

and therefore in evaporation. There is a good correlation between latent heat flux and mixed layer depth at every station in the Mediterranean Sea.

From Fig. 26 on page 44 and Fig. 24, the wind speed becomes largest between November and March. Mixed layer depth also reaches its deepest value of 197 m at this same time period in the eastern Mediterranean.

Between May and October, mixed layer depths are at a minimum, with buoyant damping associated with strongly positive Q_0 exceeding the buoyant production due to evaporation. In the case of no entrainment, $W_e = \partial h/\partial t = 0$, and $B_0 = G_0$,

$$[\alpha g(\frac{Q_0}{\rho} C_p) - \beta g \overline{S}(E - P)]h = G_0.$$

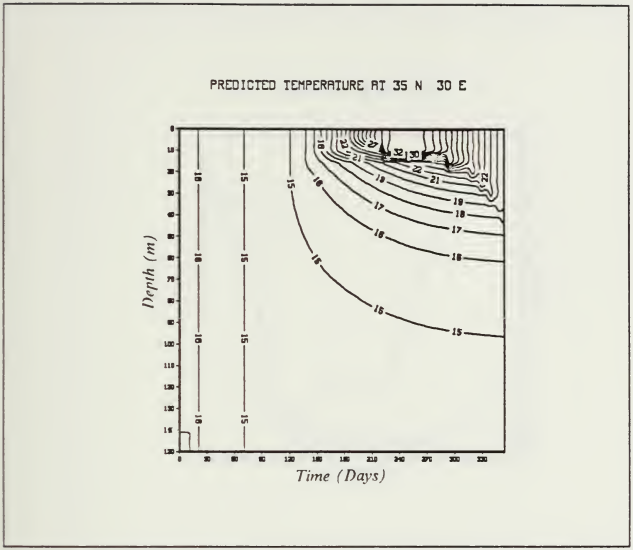

Fig. 25. The Predicted Temperature With Wind And Heat Fluxes Only

Therefore the second term on the left-hand side is small enough to make the equation (2.38) positive. The deepening in the mixed layer which is caused by wind forcing is almost the same as the deepening caused by the evaporation effect between February and April. However, between October and January, the deepening in the mixed layer caused by evaporation exceeds the deepening attributable to wind stress alone at all three stations in the Mediterranean Sea. See Fig. 18 on page 36, Fig. 21

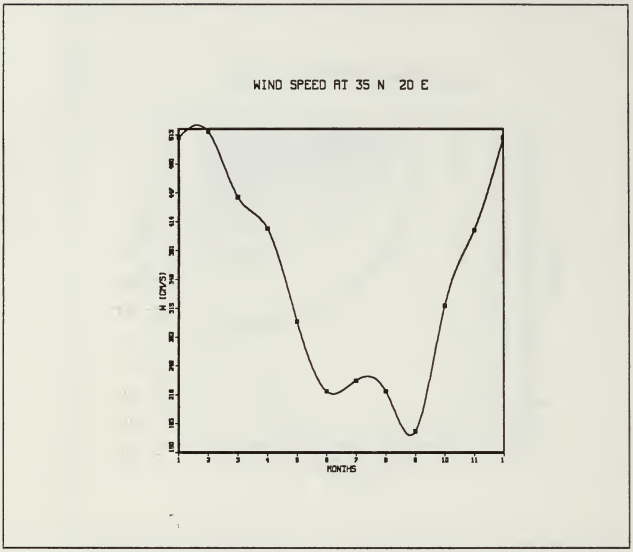

Fig. 26. The Wind Speed At 35 ° N 30 ° E

on page 39, and Fig. 22 on page 40, Fig. 24 on page 42, Fig. 27 on page 45, Fig. 28 on page 46.

Over the year, the correlation between the mixed layer depth and the surface heat flux is greater than between mixed layer depth and the evaporation rate or between the mixed layer depth and wind stress. In particular, the net heat flux minimum (November-April) and maximum (May-October), coincide well with the corresponding extremes in the mixed layer depth.

In January-April the mixed layer depth figures show clearly the domination of evaporation effects over the wind effect. This is due to strong evaporation rate over the Mediterranean Sea. This mixing caused by winds is both free and forced. The resultant

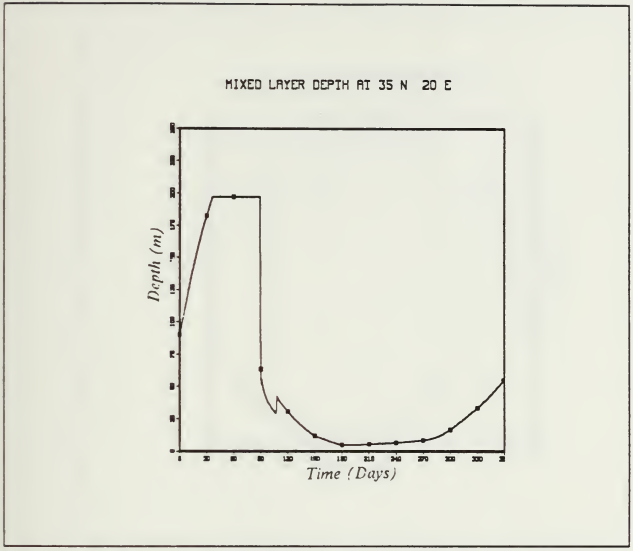

Fig. 27. The Mixed Layer Depth With Wind And Heat Fluxes Only

mixed layer depth is potentially very large, and can be a cause of intermediate and deep water formation.

In the case without wind mixing, the mixed layer depth shallows to a 2 m depth in summer time. Thus the summer wind is important in mixing the surface layer, and can not be neglected. This is due to the domination of Q_0 over E-P in equation (2.39). In that case the evaporation process becomes less insignificant for determining h.

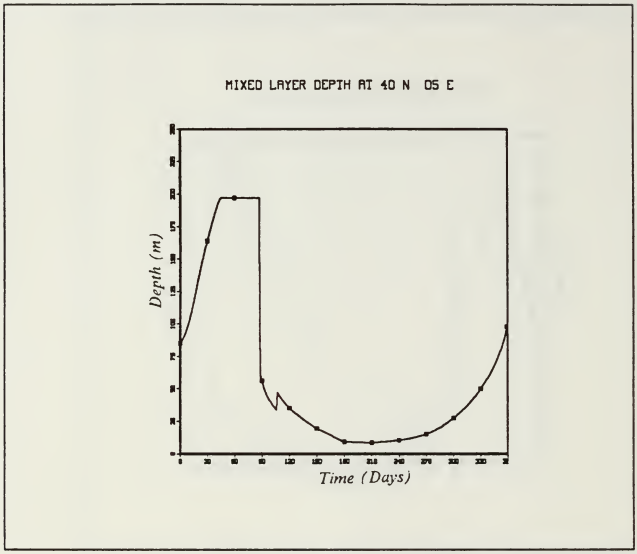

Fig. 28. The Mixed Layer Depth With Wind And Heat Fluxes Only

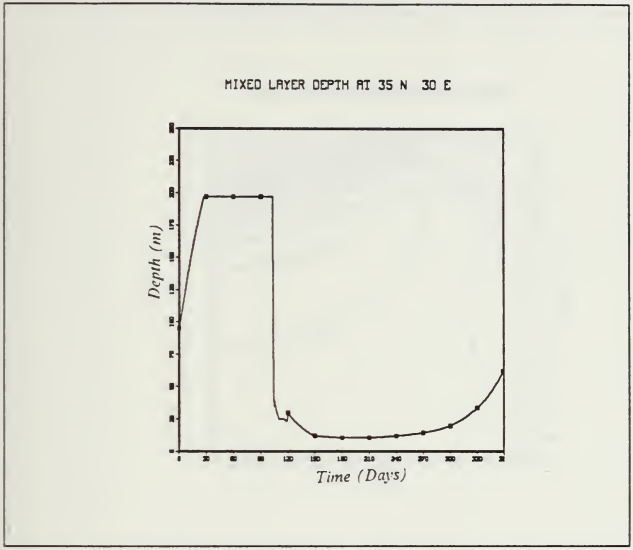

Fig. 29. The Mixed Layer Depth With Free Convection Plus Forced Convection

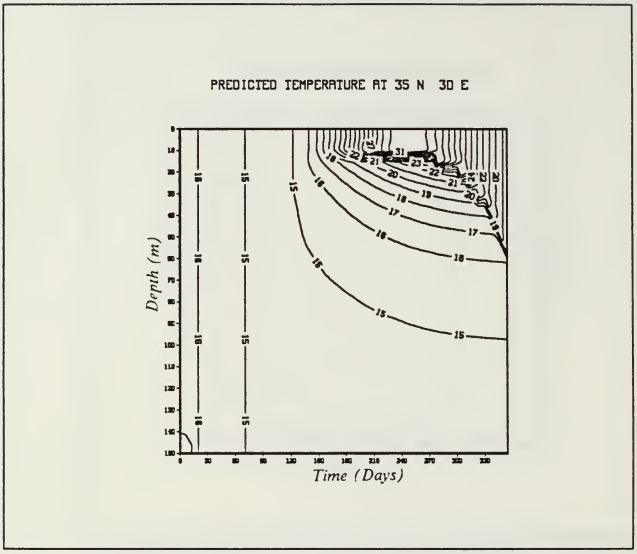

Fig. 30. The Predicted Temperature With Free Convection Plus Forced Convection

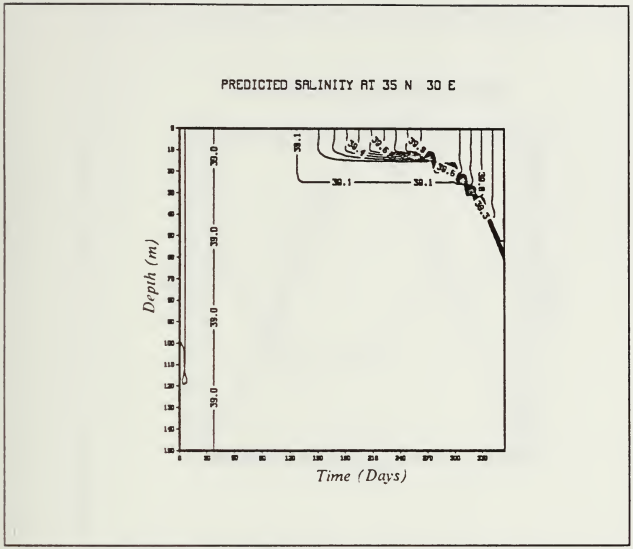

Fig. 31. The Predicted Salinity With Free Convection Plus Forced Convection

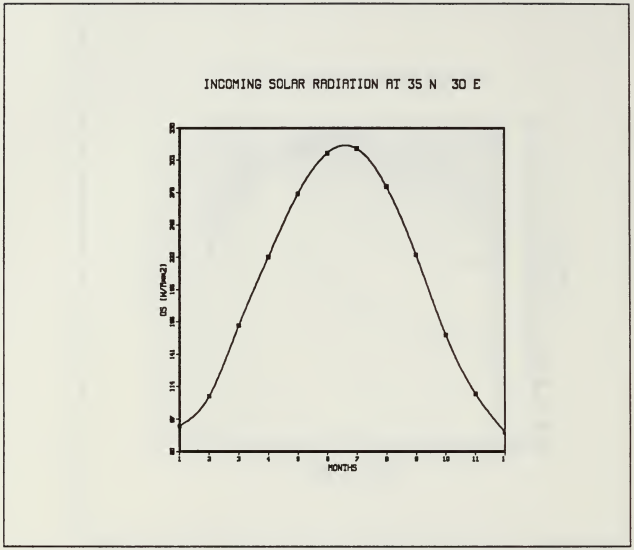

Fig. 32. The Incoming Solar Radiation At 35 ° N 30 ° E

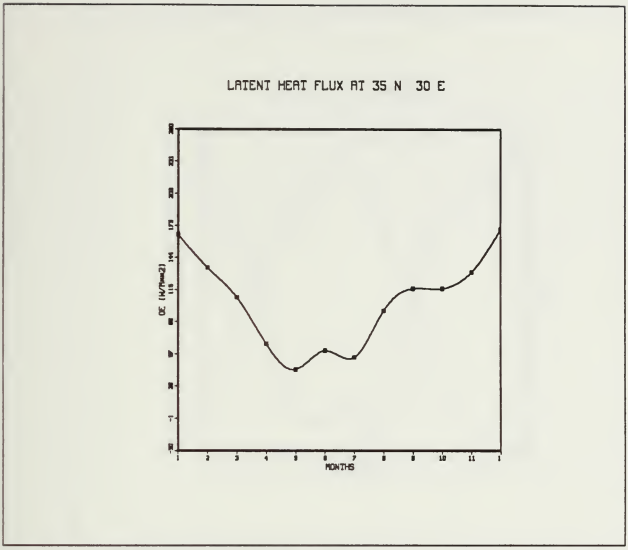

Fig. 33. The Latent Heat Flux At 35 ° N 30 ° E

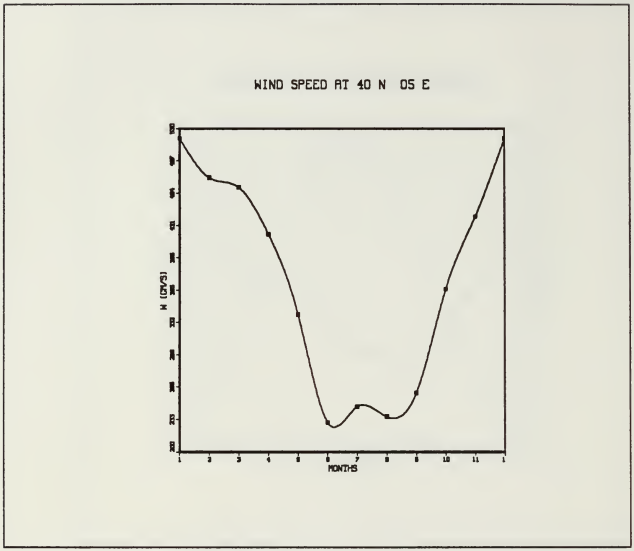

Fig. 34. The Wind Speed At 40 ° N 05 ° E

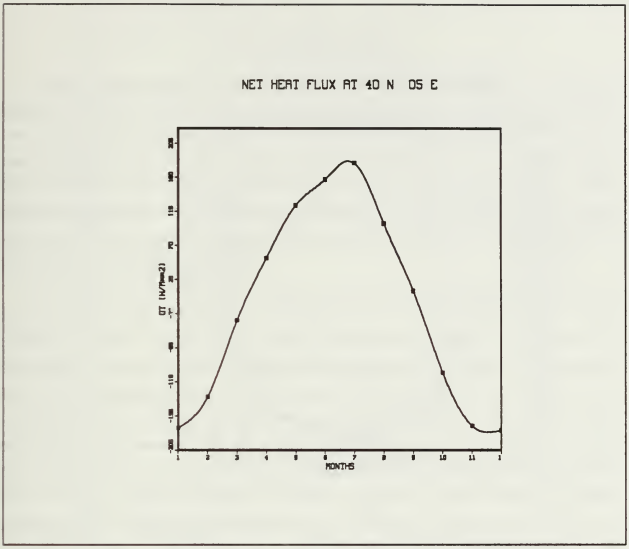

Fig. 35. The Net Heat Flux At 40 ° N 05 ° E

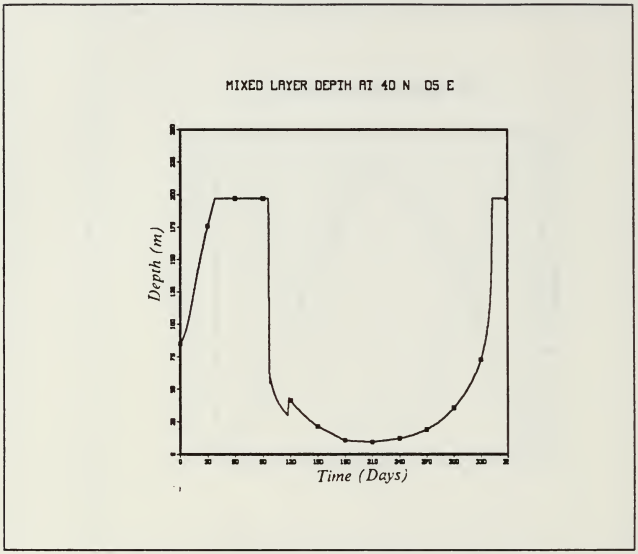

Fig. 36. The Mixed Layer Depth With Free Convection Plus Forced Convection

V. CONCLUSIONS

In this study the OPBL model was employed in order to determine the effects of seasonally varying variables on the mixed layer dynamics. The surface heat flux, wind stress, and evaporation rate are provided from the climatological data. For a variety of cases, the model is solved numerically to obtain mixed layer depth, mixed layer temperature and salinity, below-layer temperature and salinity profiles for a whole year. Three numerical experiments are conducted to demonstrate the relative roles of wind mixing, heat flux and evaporation in determining the seasonal evolution of the mixed layer at three sites in the Mediterranean Sea.

In the case of free convective mixing only (first case), evaporation and surface cooling processes can deepen the mixed layer to 197 m in January in the eastern Mediterranean Sea. Free convection and heat flux alone can deepen the mixed layer to same depth in the central and western Mediterranean as in the eastern Mediterranean. Over the summer period, free convection and heat flux alone can not explain the observed mixed layer depth for all three locations in the Mediterranean Sea. In the fall and early winter, free convection in the eastern Mediterranean Sea can deepen the mixed layer to 60 m depth. In the central and western Mediterranean such deepening reaches 90 m and 125 m depths respectively. Therefore, in general, the fall mixed layer salinity increases and the temperature decreases due to excessive evaporation rate over the Mediterranean Sea. Then in winter the layer entrains the less saline lower layer, balancing the salinity increase caused by evaporation. The positive buoyancy flux caused by increased turbulent kinetic energy due to strong evaporation starts the mixing process in fall and winter.

When the wind is a dominant mechanism, in the case of setting net evaporation to zero (second case), the results show that the mixed layer deepening reaches 197 m in late winter at all three stations.

Therefore, from the first and second cases in late winter until April, the wind and evaporation have almost the same effects on the mixed layer deepening. Ih fall and early winter until January, the evaporation process is dominant, and this is especially true in the western Mediterranean Sea.

This experiment showed that the evaporation is weakest in summer, and is most significant in late fall and in early winter. The effect of wind mixing is much more con-

tinuous in time and space than is the effect of evaporation. There are no significant wind effect differences between the three stations.

This study shows that for the seasonal time scale, evaporation is an important driving mechanism for mixed layer deepening in the Mediterranean Sea.

It is recommended that this research be continued, with an emphasis on the forcing attributable to storms and shorter-period fluctuations in the surface forcing.

REFERENCES

Bryden, Harry L., Stommel, Henry M.,1983 : "Limiting Processes That Determine Basic Features of The Circulation in The Mediterranean Sea." *Oceanologica Acta*, 7, 289-296.

Bryden, Harry L., Stommel, Henry M., 1982: "Origin of the Mediterranean Outflow."*J.Mar.Res.,Suppl.*, 40, 55-71.

El-Gindy, Ahmed A.H., El-Din, S.H. Sharaf, 1985 : "Water masses and circulation patterns in the deep layer of the Eastern Mediterranean." *Oceanologica Acta*, 9, 239-248.

Garrett, C.J.R., 1982 : "Variable sea level and strait flows in the Mediterranean: a theoretical study of the response to meteorological forcing." *Oceanologica Acta*, 6, 1,79-87.

Garwood, R.W., 1977: "An oceanic mixed layer capable of simulating cyclic states." *J. Phys. Oceanogr.*, 7, 455-468.

Garwood, R.W., Muller, P., 1988: Mixed Layer Dynamics: "Progress and New Directions." *Transactions of the American Geophysical Union* 69, 2-12.

Gascard, J.C., 1977: "Mediterranean deep water formation baroclinic instability and oceanic eddies." *Oceanologica Acta*, 1, 315-330.

Hsiung, J., 1983: "Large scale sea-air energy fluxes and global sea surface temperature fluctuations." *Ph.D. thesis, MIT, 240pp.*

Hsiung, J., 1985: "Estimates of global oceanic meridional heat transport." *J. Phys. Oceanogr., 15, 1405-1413.*

Katsaros, Kristina B., 1977: "Turbulent Free Convection in Fresh and Salt Water: Some Characteristics Revealed by Visualization." *J. Phys. Oceanogr.*, 8, 613-626.

Lacombe, H.; Gascard, J.C.; Gonella, J.; Bethoux, J.P., 1980: "Response of the Mediterranean to the water and energy fluxes across its surface, on seasonal and interannual scales." *Oceanologica Acta* , 4, 247-255.

Malonette P.- Rizzoli; Robinson, Allan R., 1988: POEM: Physical Oceanography of the Eastern Mediterranean. *EOS*, 4, 195-205.

Manzella, Giuseppe M.R., 1983 : "Fluxes across the Corsica Channel and coastal circulation in the East Ligurian Sea. North-Western Mediterranean." *Oceanologica Acta*, 8, 29-35.

Miller, James R., 1974: "The Salinity Effect in a Mixed Layer Ocean Model." *J. Phys. Oceanogr.*, 6, 29-35.

Millot, Claude, 1986: "Circulation in the Western Mediterranean Sea." *Oceanologica Acta*, 10, 143-149.

Pickard, George L. Emery, William J., 1982: *Descr. Phys. Oceanogr.* 4th Enlarged Edition, 164-167, 53-54.

Pollak, M.J., 1952: "The Sources of the Deep Water of the Eastern Mediterranean Sea." *J. Mar. Res.*, 10, 128-152.

U.S. Navy Marine Climatic Atlas of The World, 1955: 1, North Atlantic Ocean.

INITIAL DISTRIBUTION LIST

		No. Copies
1.	Defense Technical Information Center Cameron Station Alexandria, VA 22304-6145	2
2.	Library, Code 0142 Naval Postgraduate School Monterey, CA 93943-5002	2
3.	Lt.Ahmet Turker Navigation, Hydrography and Oceanography Department Cubuklu-Istanbul-Turkey	2
4.	Commender Navigation, Hydrography and Oceanography Department Cubuklu-Istanbul-Turkey	1
5.	Chairman (Code 68Co) Department of Oceanography Naval Postgraduate School Monterey, CA 93943-5000	1
6.	Chairman (Code 68Mr) Department of Oceanography Naval Postgraduate School Monterey, CA 93943-5000	1
7.	Chairman (Code 63Rd) Department of Meteorology Naval Postgraduate School Monterey, CA 93943-5000	1
8.	Prof. R. W. Garwood (Code 68Gd) Department of Oceanography Naval Postgraduate School Monterey, CA 93943-5000	2
9.	Prof. P. Chu (Code 68Cu) Department of Oceanography Naval Postgraduate School Monterey, CA 93943-5000	1
10.	Director Naval Oceanography Division Naval Observatory 34th and Massachusetts Avenue NW	1

Washington, DC 20390

11. Commander 1
Naval Oceanography Command
NSTL Station
Bay St. Louis MS 39522

12. Commanding Officer 1
Naval Oceanographic Office
NSTL Station
Bay St. Louis, MS 39522

13. Commanding Officer 1
Fleet Numerical Oceanography Center
Monterey, CA 93943

14. Commanding Officer 1
Naval Ocean Research and Development Activity
NSTL Station
Bay St. Louis, MS 39522

15. Office of Naval Research (Code 1122PO) 1
800 N. Quincy Street
Arlington, VA 22217

16. Commanding Officer 1
Naval Environmental Prediction Research Facility
Monterey, CA 93943

17. Chairman, Oceanography Department 1
U.S. Naval Academy
Annapolis, MD 21402

18. Scientific Liaison Office 1
Office of Naval Research
Scripps Institution of Oceanography
La Jolla, CA 92037

19. Commander 1
Oceanographic Systems Pacific
Box 1390
Pearl Harbor, HI 96860

20. Commanding Officer 1
Naval Eastern Oceanography Center
Naval Air Station
Norfolk, VA 23511

21. Commanding Officer 1
Naval Western Oceanography Center
Box 113
Pearl Harbor, HI 96860

22. Commanding Officer
Naval Oceanography Command Center, Rota
Box 31
FPO New York, NY 09540 1